1990 SCA CONFERENCE PAPER NUMBER 9003

DIRECT MEASUREMENT OF THE CONSTITUENT POROSITIES IN A DUAL POROSITY MATRIX

Robert M. Moss: Texaco Inc., Houston, Texas
Gregory P. Pepin: Texaco Inc., Houston, Texas
Lorne A. Davis: Texaco Inc., Houston, Texas

Abstract: A direct measurement of core porosity by x-ray computed tomography (CT) has been used to determine the storage capacities (porosities) of several dual porosity systems. A contrast agent, time sequenced scanning, and image subtraction techniques are used to measure the porosities of both components of a dual porosity system. The method requires no knowledge of core mineralogy or assumptions about fracture width.

To perform the measurement, a clean, dry, evacuated core contained in an aluminum pressure vessel is scanned. Then a single location in the sample is scanned repeatedly after introducing a radiopaque fluid. After the system comes to equilibrium, the saturated core is re-scanned. Subtraction of the evacuated images from the invaded images, after scaling, provides quantitative porosity images. The porosity of narrow fractures, which may be invisible to a thresholding technique, can be quantified. This sequential scanning procedure can determine fracture/matrix permeability ratios if the fracture permeability is an order of magnitude different than the matrix permeability.

The porosity images provide statistically accurate porosity distributions. The width of the porosity distribution is a good indicator of porosity heterogeneity. The mean of the distribution agrees very well with helium porosity measurements. Data from samples of Monterey shale, Bakken shale, and coal are used to illustrate the method.

INTRODUCTION

Fracture porosity and permeability are of great interest because of their effects on hydrocarbon capacity and producibility of highly fractured reservoirs. Previously published techniques for detecting fractures in whole core samples include methods such as epoxy impregnation of the core and CT measurements in which a contrast agent is injected into the sample prior to scanning (Bergosh and Lord, 1987). The first method is destructive. The second requires an assumption of the fracture width, and the contribution to the porosity of very small fractures is missed because of the thresholding method used. We present here a method of measuring the constituent porosities of dual porosity systems which uses an X-ray contrast agent along with multiple X-ray computed tomography (CT) scans of a core to obtain direct measurements of the porosity. Unlike estimates made using single scans, this technique requires no assumptions of either fracture width or core mineralogy. In the following, the methods used to measure porosity and to detect dual porosity using CT are described. The effects of several experimental variables on the statistics and errors of the measurement are examined. Finally, data from three fractured samples are provided as examples of the technique.

POROSITY DETERMINATION USING X-RAY CT

Porosity can be determined from X-ray CT measurements using either single-scan or multiple scan techniques. A few authors have described measurements of porosity from single scan techniques, usually in homogeneous samples such as Berea sandstone (Wellington et al.,1987; Withjack, 1988). Correlations between CT number and porosity were mentioned by Hunt et al. (1988). To our knowledge the present paper provides the first published data on the direct measurement of porosity and fracture porosity using a two-scan CT method.

Because a core consists of the rock matrix and a fluid or gas filled pore system, the measured CT number is made up of

contributions due to both the rock (mineralogy) and the porosity. A simple equation describes the relationship:

$$CTN_m = (1-\phi)*CTN_r + \phi*[S_o*CTN_o + S_b*CTN_b + S_g*CTN_g] \quad (1)$$

In equation 1, the CT number (CTN) is in Hounsfield units, the standard scale used in the medical industry. In Hounsfield units, the CTN for air is -1000 HU and the CTN for water is 0 HU.

Two major benefits of single scan estimates of the porosity are that they can be made using native state cores and are faster than two-scan measurements. However, accurate measurements require independent knowledge of small scale variations in core mineralogy and fluid saturations. Porosity estimates made without this knowledge require several simplifying assumptions: an assumption of the core mineralogy; an assumption of gas and liquid saturations; and an assumption of CTN's of the fluids. A large source of error in these porosity estimates lies in the assumption of known lithology. Different cementing or clay minerals dispersed throughout the rock matrix will affect CTN_r, and if they are not accounted for in estimating the matrix CTN, an erroneous estimate of the porosity can result.

In the two-scan technique, CT scans are made at the same physical location in a core at different, known fluid saturations. The porosity at each location can be determined directly by performing a pixel by pixel subtraction of the two images and dividing by a calibration constant. If the two conditions are dry and evacuated ($S_f = 0$), and fluid saturated ($S_f = 1$) then equation 1, determined for the two saturation conditions, can be used to determine the porosity:

$$\phi = \frac{CTN_f^c - CTN_v^c}{CTN_f - CTN_v} \quad (2)$$

This method removes any contribution due to the rock, negating the need for mineralogy information. In addition, the image subtraction technique greatly reduces the effect of beam hardening artifact on the final results. Two drawbacks are the need to clean and dry the sample and the additional time needed for the experiment. The only limitation that the CT measurement places on the saturating fluid is that it must have a CT number much larger than the CTN of vacuum, which is essentially the CTN of air at one atmosphere (-1000 HU). Common oilfield liquids, such as crude or refined oils or brines, can be used. Due to the low x-ray absorption coefficients of hydrocarbon gases, xenon or some other radiopaque gas is needed if the sample is to be saturated with gas. Figure 1 compares the porosity measured using this technique to the porosity measured using a helium porosimeter for a number of different core plugs. The figure includes data points from Berea sandstone, various carbonates, and EP Porous Structures Grade 15 (trademark of Eaton Products International Inc.). The saturating liquid for these CT measurements was a refined mineral oil. The CT porosities agree well with the helium porosities.

The usefulness of the dual-scan CT porosity measurement does not lie in its ability to determine the average porosity of a clean, dry core sample; this can be done more quickly using a helium porosimeter. The power of the CT measurement is its ability to visualize the distribution of the porosity on a very small scale. The images of porosity allow visualization of the spatial distribution of high or low porosity streaks or fractures. The porosity of these features can be determined quantitatively without having to assume their width. The porosity images can be analyzed to create histograms of porosity, either for an entire core or for a single 'slice' of the sample. We have found these distributions to be valuable for analyzing dual-porosity and fractured systems.

MEASUREMENT OF DUAL POROSITY AND FRACTURE POROSITY

Two techniques were studied to measure dual porosity and fracture porosity systems: dynamic scans and porosity histograms. The dynamic scan technique can detect permeability differences larger than an order of magnitude in dual porosity systems. An example would be fractured shale samples consisting of a low permeability matrix and a higher permeability fracture system. Porosity histograms allow statistically accurate measurement of the porosity, as well as providing a porosity distribution.

Dynamic scanning is a fast scanning technique available only on CT scanners with short scan times, such as fourth generation scanners. Dynamic scans can be performed on only one location in the sample at a time. A clean, dry core sample is placed within a core holder and evacuated. The evacuated sample is scanned at a single location of interest for the dynamic experiment. A radiopaque gas or fluid is then injected into the core, either radially or along the axis. During the fluid injection, multiple scans of the core are made to obtain time sequenced images of the fluid invasion. Short scan and interscan times are needed to visualize the filling of the higher permeability pore/fracture system. Time sequenced images of invaded pore space can be created using equation 2. If the two pore systems have significantly different permeabilities, they will fill at noticeably different rates. This will be seen either in the porosity images or by analyzing the rate of increase in the average "invaded" porosity.

The second technique uses porosity histograms. The distributions are simply frequency histograms of the porosity within a region of interest selected in a porosity image. In general the porosity distributions that we discuss are distributions over bulk volume, and are not normalized to pore volume. Regions can be chosen to encompass an entire axial slice image or any subset of the image so that specific features within the sample, such as fractures, can be targeted. The porosity distribution within an

entire core can be determined by adding all of the slice by slice porosity histograms obtained from scanning the core. Figures 2a - 2c show some whole sample porosity histograms measured for cores used for Figure 1. Figure 2a is EP Porous Structures Grade 15, a man-made porous material with a uniform pore diameter of about 15 microns. Figure 2b is a homogeneous carbonate and 2c is a very heterogeneous, dual porosity carbonate. The data show that the standard deviation of the porosity histogram is a good indicator of porosity heterogeneity in a core.

EXPERIMENTAL DETAILS

A fourth generation Technicare 2060 CT scanner was used to perform the experiments. All measurements were made at room temperature. Scan parameters were 120 kVp x-ray tube voltage, 2 mm slice thickness, and 12.5 cm scan diameter. The scan time and x-ray tube current varied. All data were taken with the scanner calibrated using a synthetic ceramic phantom with a CT number between sandstones and carbonates. This rock tune-up greatly reduces beam hardening artifacts in the images. Image array size is 512 x 512, with each pixel representing a volume element 0.25mm x 0.25mm x 2mm. Minimum spatial resolution was 0.5mm x 0.5mm x 2mm; of course, features smaller than the voxel size can be detected if the CT number contrast with surrounding material is sufficiently large. The resulting images were analyzed on a MicroVAX 3800 (trademark of Digital Equipment Corporation) with special hardware for image display. Specialized software for the quantitative analysis of core image data was developed in-house using the IDL programming language.

To perform the porosity measurements a clean, dry core was suspended within a thin-walled aluminum pressure vessel and evacuated. A series of scans was made of the entire evacuated core at 2 mm intervals to ensure complete coverage of the sample. Using the evacuated images, a single location was selected for the dynamic scans. A series of scans was made at that location as xenon gas was injected into the sample. Because there was no

confining pressure, the gas entered the sample from all directions, similar to a helium porosity measurement. Interscan times varied from 15 to 30 seconds at the start of an experiment to several hours towards the end. Small interscan times were needed at the beginning to detect the filling of high permeability fracture systems. For very low permeability shale samples, several days were needed for complete filling of the matrix to occur. At the end of the dynamic series, the entire saturated core was rescanned so that porosity images of the whole sample could be obtained.

The gas injection pressure was monitored using a Sensotec pressure transducer and controlled by a computer controlled solenoid valve in order to maintain a constant pressure throughout the experiment. In addition, a TTL level high voltage control signal from the CT scanner was used as a computer interrupt to allow pressure readings and elapsed times to be obtained for each scan.

To obtain the porosity for both dynamic and whole core samples, a pixel-by-pixel subtraction was made of the evacuated sample image from the corresponding image of the saturated sample. This provided the numerator for equation 2. The denominator was obtained by scanning the empty aluminum vessel before (evacuated) and after filling with xenon at the same pressure that was used to saturate the core. The vacuum image was subtracted from the xenon image, and the average was used to obtain the calibration constant for converting the subtracted core images to porosity images.

While the basic technique described above is fairly straightforward, a number of errors can be introduced into the data if the experimental conditions are not carefully controlled. Two factors which control the statistical quality of the images are the scanner setup (scan time, tube current, slice thickness) and the core barrel material and thickness. These control the x-

ray flux that is incident on the core sample, affecting the minimum standard deviation of the porosity histogram. If the core barrel is too dense or too thick or the x-ray current is too low, a large spread in the porosity histogram due to low statistics will result. Figure 3 compares the standard deviations in the CT number for a fuzed quartz sample scanned with varying scan times and tube currents through both aluminum and titanium core barrels. The increase in the standard deviation seen at the small scan time and through the titanium core barrel can mask useful information in the porosity distribution. These data indicated that 8 second scan times through the thin (0.125 inch) aluminum barrel would minimize the statistical spread in the data.

Measurement errors can also be caused by the addition of the saturating fluid between the two sets of core scans. Fluids can affect the measured CTN of the saturated sample due to the increased beam hardening caused by the addition of fluid into the annulus between the outside surface of the core and the inside of the core barrel. If the annulus is thick, the significant amount of additional beam hardening through the fluid can reduce the measured CTN of the saturated core, resulting in an underestimate of the porosity. To avoid this problem, the thickness of the annulus should be minimized by matching the ID of the core barrel to the diameter of the core sample. A spacer can be used for small or odd sized samples.

The porosity measurement is also affected by beam hardening through the core itself. The change in the amount of beam hardening between an evacuated sample and the same sample saturated with an x-ray absorbing fluid results in a minimum spread in the porosity distribution. To test the magnitude of this effect, a set of very homogeneous aluminum standards with different CT numbers was scanned. The standards were chosen to have CT numbers similar to those for evacuated and saturated core samples. The images of the different standards were subtracted

from one another to obtain images analogous to porosity images, and the subtracted images were analyzed to determine the mean ΔCTN and standard deviation. Because of the homogeneity of the samples and the good statistical accuracy of the images, the standard deviation was primarily an indicator of the different amounts of beam hardening through the samples with different CT numbers. The standard deviations were, on average, 4.5% of the mean of the ΔCTN distribution. This says that for a completely homogeneous sample, the measured porosity distribution will be gaussian in shape and will have a standard deviation of about 4.5% of the mean due to beam hardening effects. Other features in the distributions of heterogeneous core must be due to actual variations in the porosity distribution. The EP Porous Structures Grade 15 sample (Figure 2a) was used to confirm this result. The standard deviation ($\Delta\phi$=1.3%) is 4% of the mean (ϕ=32.7%), in good agreement with the expected minimum spread caused by beam hardening.

EXAMPLES OF THE TECHNIQUE

MONTEREY SHALE

The Monterey shale is a relatively impermeable matrix/fracture system. The core used for the experiments was a whole core approximately six inches long which contained a number of thin bedding planes with varying densities and small fractures. The scan time was 2 seconds with a tube current of 100 mA. This combination of scan parameters results in the noisiest images of all scan techniques. However, it does allow scans every 15 seconds at the beginning of the series, which can be important when visualizing high permeability fractures. Figure 4 shows the evacuated CT number image at the dynamic scan location and a corresponding porosity image after several days were allowed for the sample to become fully saturated. The variation of the porosity between the porous fractures and matrix and non-porous thin beds are visible.

The rate of xenon invasion into the sample was determined for several regions of interest (ROIs), which are highlighted in Figure 5. The mean porosity as a function of time for the ROIs is plotted in Figure 6. The time axis in the figure is logarithmic. ROI 0 encompassed the entire slice. The gas in the annulus did not reach its nominal 95 psig until the eighth data point (139 seconds). It is clear that the lowest CT number bed (ROI 3) is significantly more permeable than the other parts of the sample. The porosity for ROI 1 drops below 0 at small times due to the beam hardening through the annulus and through the gas-filled core. The flattening of the porosity curve for ROI 3 and ROI 4 indicates that those regions have essentially completely filled by the end of the experiment. The endpoint for ROI 3 gives a porosity of 26.5% for the high permeability part of the slice. The curves for the other ROI's show that complete filling of these regions will take a long time.

Figure 7 shows a normalized frequency histogram of the porosity distribution obtained for the dynamic scan location at the end of the experiment. The dual porosity nature of the sample is indicated by the bimodal nature of the histogram. The porosity data is plotted with the two components of a dual gaussian function that fit the porosity distribution accurately.

BAKKEN SHALE

The Bakken shale sample reported on here was from a horizontal well, where fracture orientation is particularly important. This particular sample was taken from a vertical part of the well, prior to step-out. This measurement was unusual in that the core was left in the native state; the sample was neither cleaned nor dried first, as is usually the case. The sample was evacuated then filled with xenon. The scans were run with a scan time of 8 seconds and a tube current of 75 mA, resulting in better statistical accuracy and less noisy images. Time constraints required that the experiment be ended before the sample came to equilibrium.

For this experiment, two sets of data are presented showing variations in porosity along the core axis. Figure 8 shows slab images parallel to the axis of the sample. The left image is a CT number image, showing dark features that are thin, higher porosity horizontal beds. This was confirmed with the porosity image shown on the right. Note the exact correspondence between the dark, low CT number regions in the left image with the bright, higher porosity areas in the right image. The porosity variations visible in the images also show up in a plot of the porosity as a function of the position along the core axis (Figure 9), with high porosity corresponding to the white areas of the porosity slab image.

COAL SEAM GAS STORAGE

There is currently much interest in understanding the behavior of methane storage and production in coal seam reservoirs. Our technique can give a quantitative measurement of the amount of gas that can be stored within the sample. In addition, data taken as a function of time allows the determination of a fill rate.

In one of our more recent experiments, we measured the uptake of xenon gas by a coal sample over 5 days, at increasing pressures of 20, 40, and 95 psig. Xenon gas was convenient to use as a contrast agent since its molecular diameter is only 5% larger than that of methane (Sloan, 1990). We expect it to give a lower bound on methane storage by surface adsorption and hydrate formation.

A Delrin (trademark of E. I. duPont Company) spacer was custom fit to this sample and was placed inside the aluminum barrel to minimize beam hardening due to gas in the annulus. Care was taken to calibrate under the same experimental conditions, i.e. inside the aluminum barrel with the spacer in place.

Because we ran the dynamic series with an 8 second scan time and 75 mA current, the smallest interscan time allowed due to X-ray tube heating was 30 seconds. The higher beam current and long scan time significantly reduced the noise in the images. Figure 10 shows a comparison of the sample setup for the Monterey shale and the coal sample.

The first part of the dynamic series was run at 20 psig. Figure 11 shows the density image at 30 seconds and a histogram of the density image for an ROI encompassing the entire image. The values shown are gas density relative to the density of the gas in the annulus. The image is scaled between relative densities of 0 and 0.5. Note that the beam hardening in the image is negligible. This is confirmed by the fairly narrow and symmetric RMSD spread of the histogram and by the fact that no density values have been pushed less than zero by differences in the beam hardening between the evacuated and the saturated images. After 30 seconds, the mean relative density within the sample is 0.1. This gives a mean value for the fracture (high permeability) porosity of 10%.

The evacuated CT number image and the porosity image at 30 seconds are compared in Figure 12. It is clear from this figure that the fractures and some of the matrix have already started to fill, so the value of 10% is probably an upper limit on the fracture and high permeability porosity. This assumes that the fractures fill before a significant amount of adsorption takes place. Adsorption probably is already visible in a few small regions, shown in red and yellow in Figure 12.

An image of the sample after 4.3 days is shown in Figure 13. The pressure in the annulus at the time of this scan was 86 psig. The nominal pressure of 95 psig decreased over the prior weekend because of the large amount of adsorption taking place in the coal. Note that this image is scaled between relative densities of 0 and 3.0. The sample is observed to have stored within the

matrix an average of 2.9 times the density of the surrounding gas. By the time of this scan, the small red area in the image had reached its maximum value and was no longer absorbing gas at this pressure. The experiment was stopped soon after this image was obtained due to time constraints. Future experiments are planned using higher pressures and temperatures to try to mimic downhole conditions. In addition, data will be collected both as the sample fills and as it drains, allowing a comparison of filling and emptying rates.

CONCLUSIONS

1. The dual scan technique is ideal for the determination of fracture orientations, as well as the quantitative measurement of the various components of the porosity distribution of the sample.

2. Dynamic scanning can provide an indication of the ratio of the permeabilities between fracture and matrix systems if the ratio is greater than an order of magnitude.

3. Histograms of the porosity distribution can provide information on the porosity heterogeneity. Bimodal porosity distributions indicate the presence of dual porosity systems, although the inverse statement may not necessarily be true.

4. Longer scan times at higher currents (e.g. 8 second scan at 75 mA) give the clearest images. However a compromise must be struck between the noise level in the image and the speed with which the earliest scans are taken. This is scanner and sample dependent.

5. The highest quality images are obtained when the beam hardening corrections before and after the introduction of the fluid are nearly the same. This can be achieved by

minimization of the annular region and/or by prehardening the beam with an appropriate spacer around the sample.

ACKNOWLEDGEMENTS

The authors wish to thank Texaco, Inc. for permission to publish this paper. We also thank Halliburton Services for the coal sample and Core Laboratories Inc. for the use of the Bakken shale sample. We appreciate both Core Laboratories Inc. and Halliburton Services for allowing us to publish these results.

Nomenclature

CTN = CT number, Hounsfield Units
S = Saturation
CTN_f^c = measured CTN of fluid filled core
CTN_v^c = measured CTN of clean, dry, evacuated core
ϕ = porosity
HU = Hounsfield units

Subscripts:

$_m$ = **m**easured
$_o$ = **o**il
$_b$ = **b**rine
$_g$ = **g**as
$_r$ = **r**ock matrix
$_f$ = **f**luid
$_v$ = **v**acuum

REFERENCES

Bergosh, J. L. and G. D. Lord, 1987, "New Developments in the Analysis of Cores From Naturally Fractured Reservoirs", SPE-16805: Society of Petroleum Engineers, presented at the 1987 Annual Technical Conference and Exhibition, Dallas, September 27-30, p. 563-570.

Hunt, P. K., P. Engler, and C. Bajsarowicz, 1988, Computed

Tomography as a Core Analysis Tool: Applications, Instrument Evaluation, and Image Improvement Techniques: Journal of Petroleum Technology, vol. 40, no. 9, p. 1203-1210.

Sloan, E. D., 1990, Natural Gas Hydrate Phase Equilibria and Kinetics: Understanding the State-of-the-Art: Revue de L'Institut Français du Pétrole, vol. 45, no. 2, p. 245-266.

Wellington, S. L. and H. J. Vinegar, 1987, X-Ray Computed Tomography: Journal of Petroleum Technology, vol. 39, no. 8, p. 885-898.

Withjack, E. M., 1988, Computed Tomography for Rock Property Determination and Fluid Flow Visualization: SPE Formation Evaluation, vol. 3, no. 4, p. 696-704.

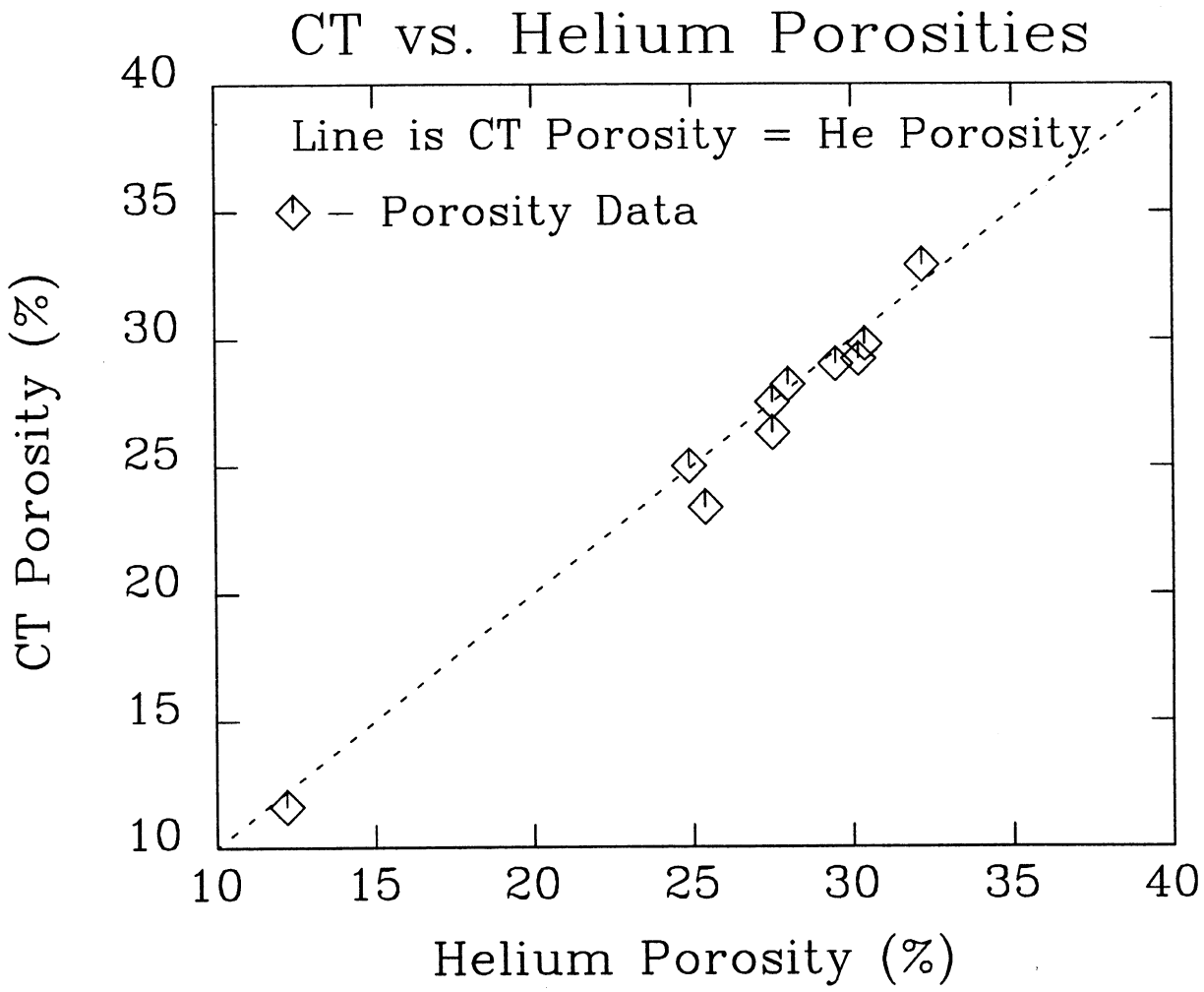

Figure 1 - Comparison of mean porosities measured on various samples using helium porosimetry and the dual scan CT method. Samples include Berea sandstone, various carbonates, and EP Porous Structures Grade 15. Ideally all data points would fall on the dotted line.

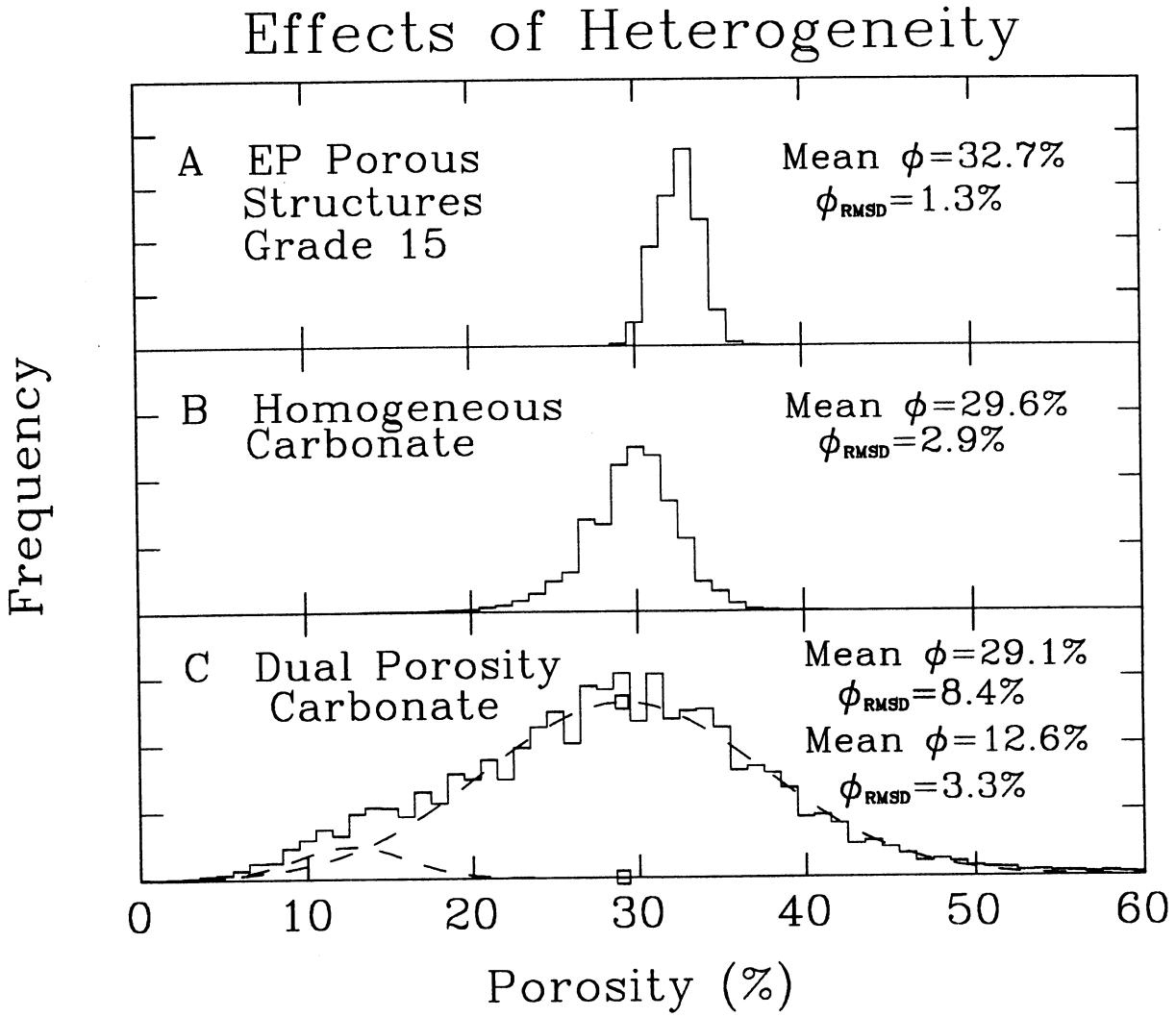

Figure 2 - The effects of porosity heterogeneity on the width of the porosity distribution is illustrated with three widely varying samples. EP Porous Structures Grade 15 is a man-made material with a uniform pore diameter of about 15 microns.

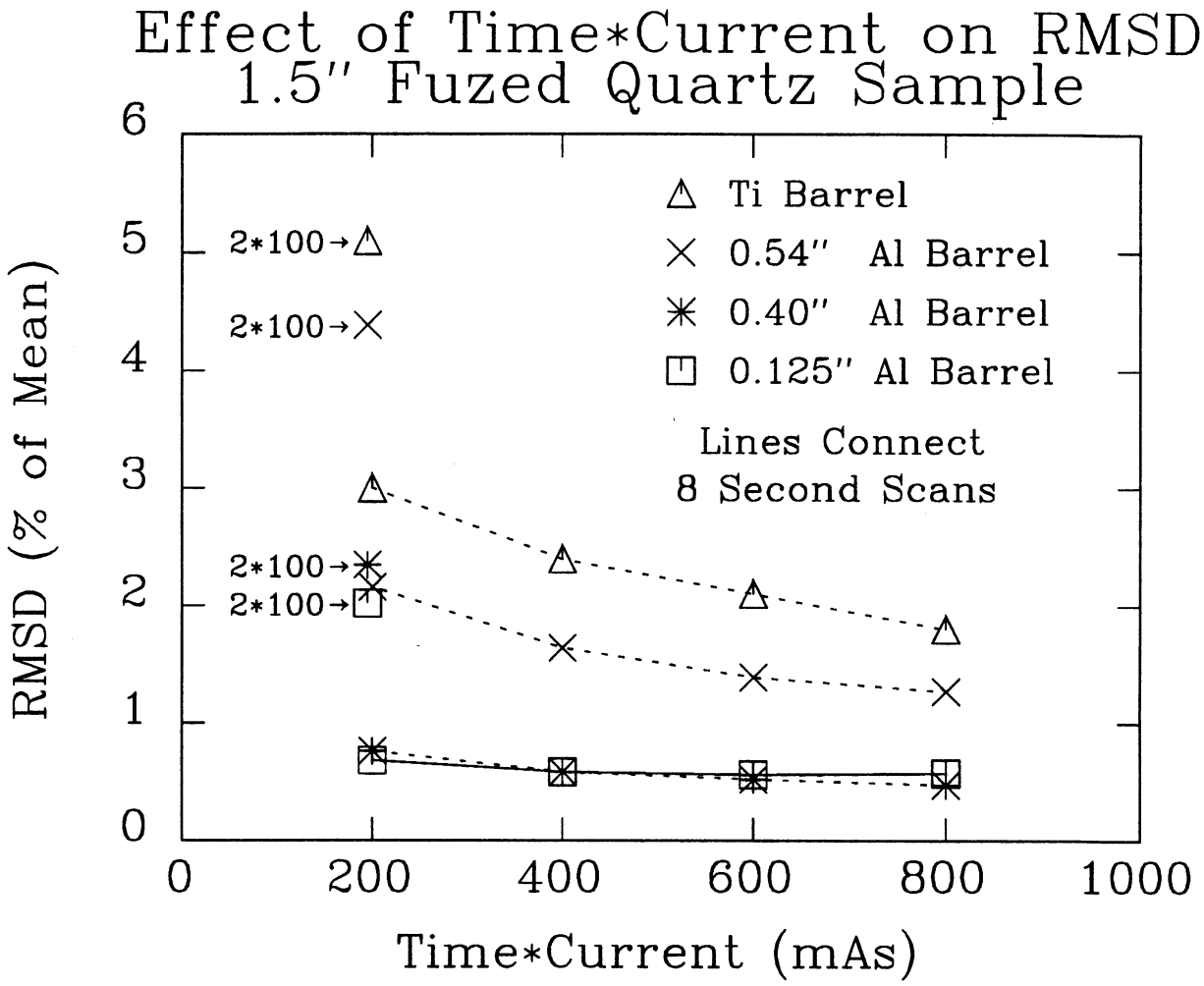

Figure 3 - The effects of scan time and beam current on the standard deviation of a fuzed quartz standard is plotted for four different pressure vessels. The ordinate is the RMSD of the measured distribution in terms of percentage of the mean value of the distribution. The 0.125 inch aluminum barrel with an 8 second scan time gave the best results.

Figure 4 - The evacuated CT number image (left) and the porosity image (right) of a slice of a Monterey Shale sample. This data was collected with a 2 second scan time, which was the primary factor in the noise level of the images.

Figure 5 - A full resolution image of the evacuated slice used for the dynamic scans of the Monterey shale sample. Regions of interest used in the analysis are outlined and numbered. ROI 0 is the circular region for the whole slice.

Figure 8 - Slab images of the Bakken shale sample reconstructed from the slice images. The resolution along the horizontal direction in these images is limited by the 2 mm slice thickness. The highest porosity areas are seen in white in the porosity image (right) and dark blue/green in the CT number image (left).

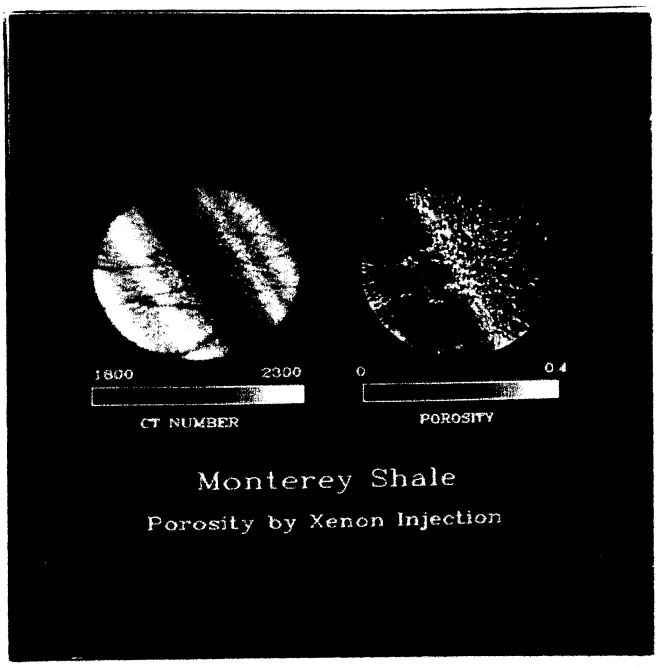

Figure 4

Figure 5

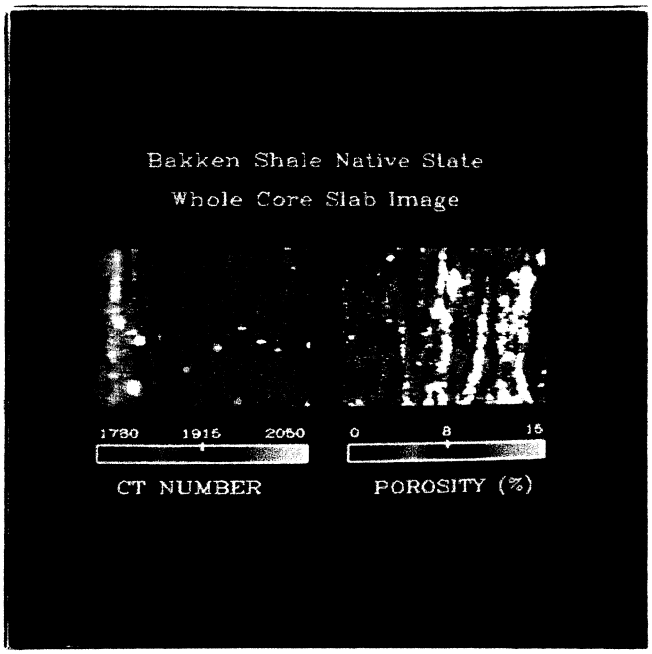

Figure 8

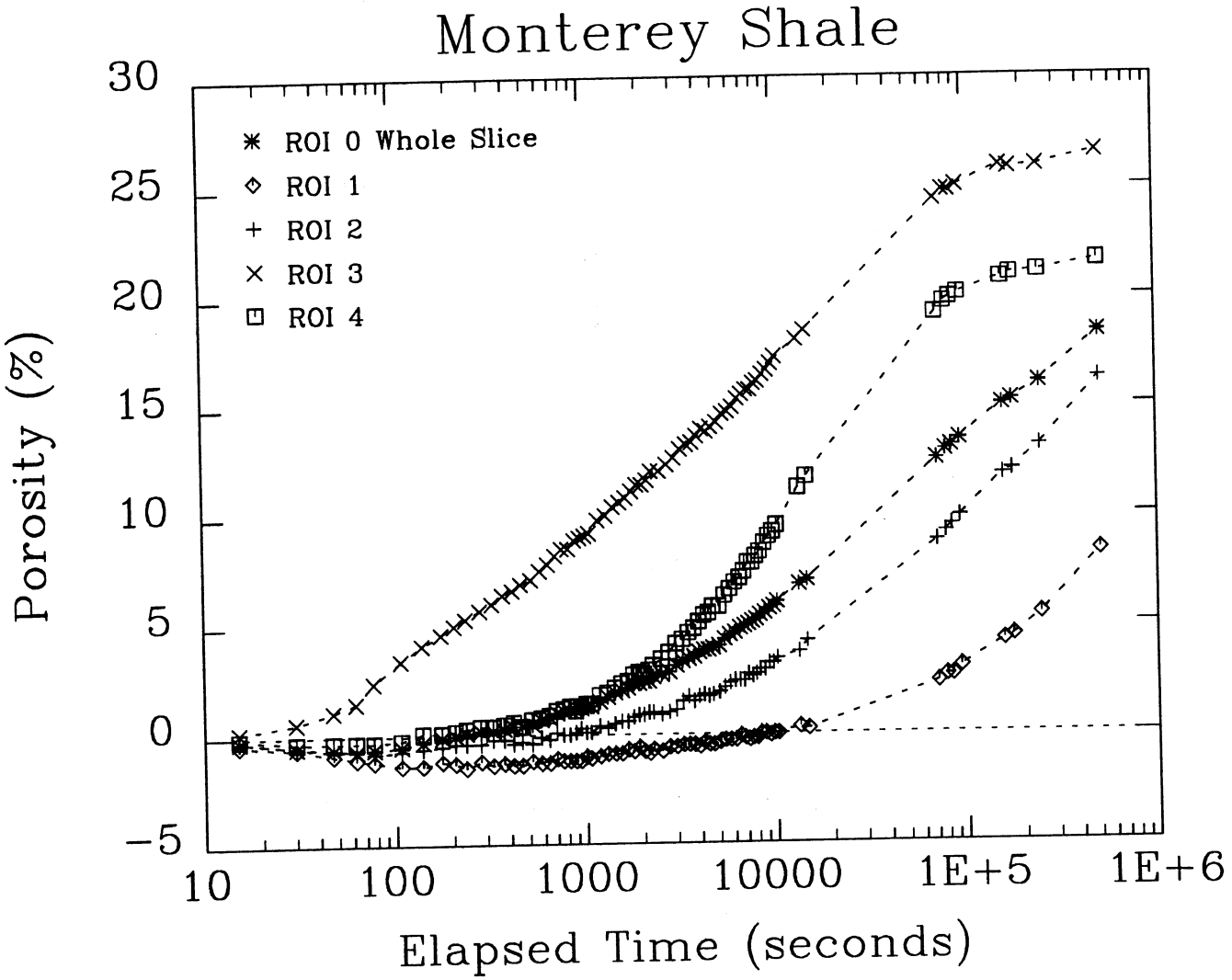

Figure 6 - Plot of the mean porosity as a function of time within the regions of interest (ROIs) shown in Figure 5. The abscissa is logarithmic. The flattening of the curves for ROI 3 and ROI 4 indicate that these regions have come to equilibrium.

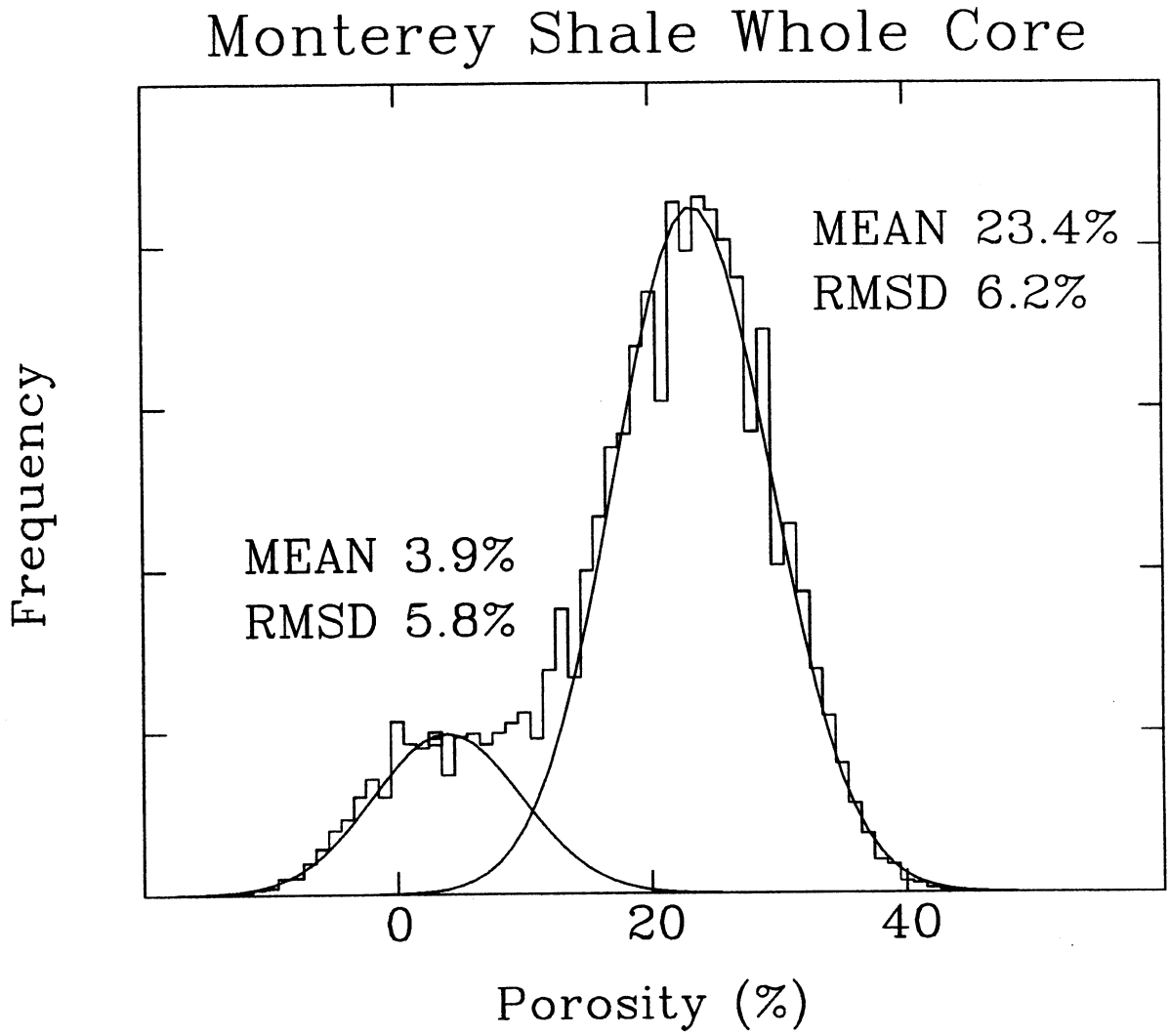

Figure 7 - The porosity distribution from the whole core porosity data for the Monterey shale sample. The dual nature of the distribution is quantified by fitting two normal distributions simultaneously to the two components of the porosity. The 2 second scan time contributed to the widths observed.

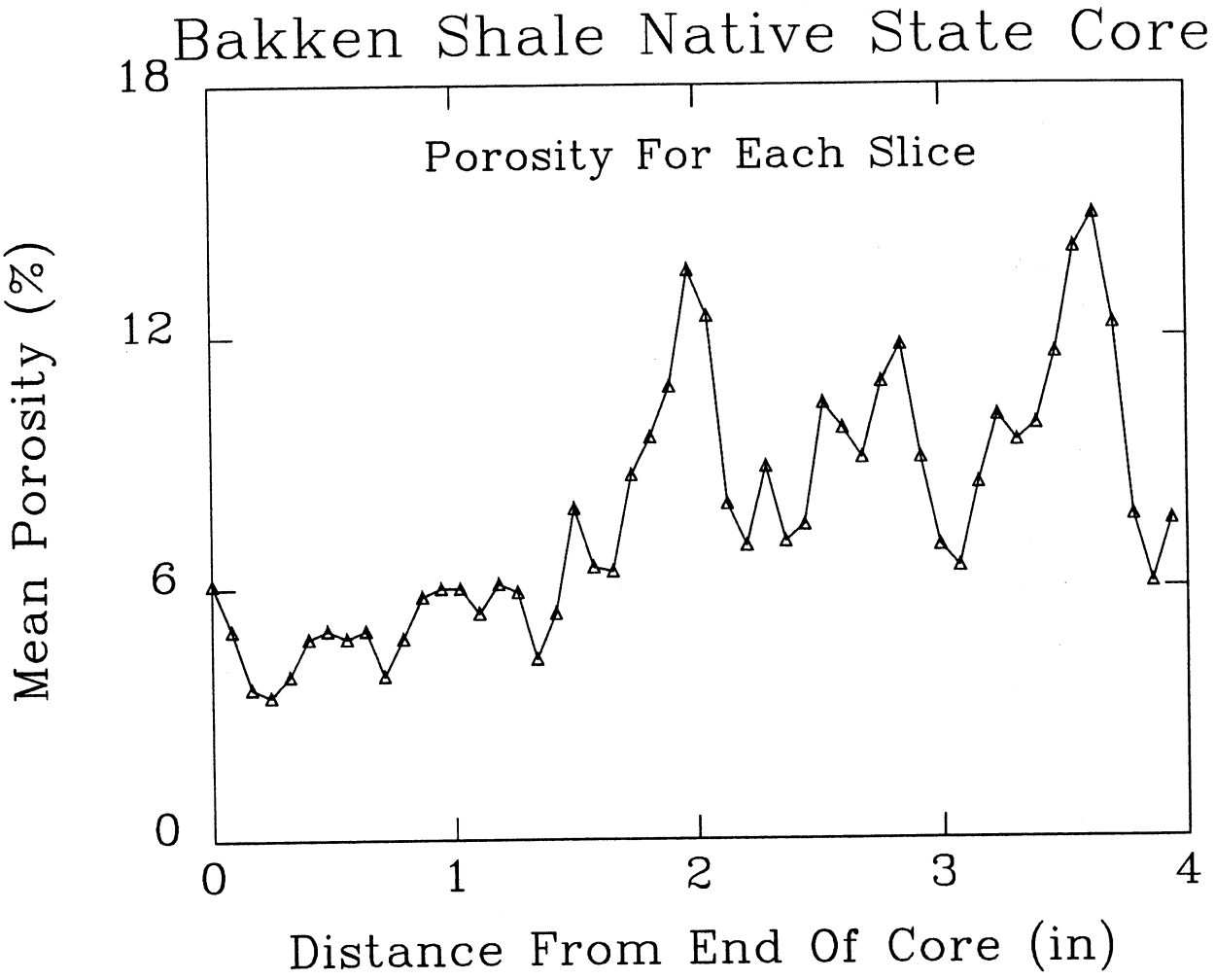

Figure 9 - The mean porosity as a function of distance from the end of the core for the Bakken shale sample. These whole core data correspond well to the individual porosity image in Figure 8.

Figure 10 - The differences in the experimental setup for the Monterey shale experiment and the coal experiment. The addition of the plastic spacer greatly reduced beam hardening by minimizing the annulus and prehardening the beam. It also helped in centering the sample.

Figure 11 - Porosity data after 30 seconds for the coal sample. The image is normalized to the gas density in the annulus (white on this scale). The fractures are already filled, and some adsorption is already taking place. The xenon gas was at 20 psig.

Figure 12 - A comparison of the evacuated CT number image (left) and the porosity image (right) after 30 seconds for the coal sample. The dark areas in the CT number image are fractures. The white areas in the CT number image are probably sand.

Figure 13 - Porosity data after 4.3 days for the coal sample. The green ring is the gas in the annulus (relative density = 1). The sample has absorbed 2.9 times the density of the surrounding gas on average. The nominal pressure at the time of this image was 86 psig.

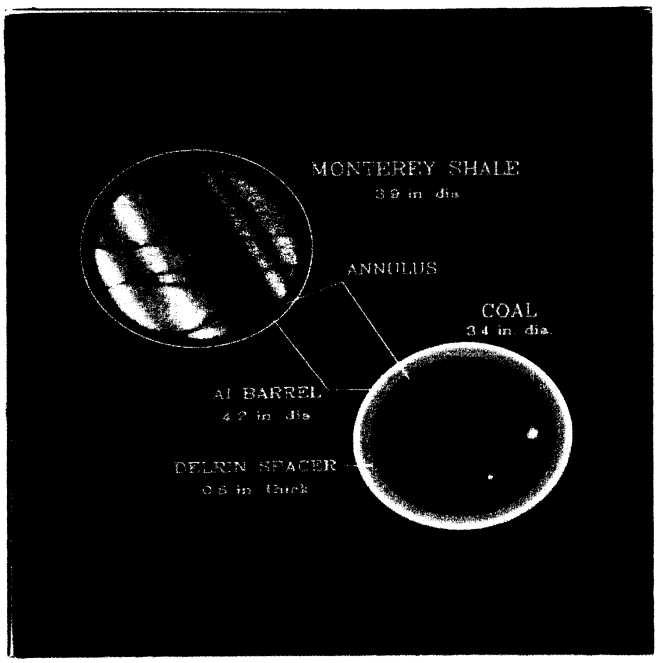

Figure 10

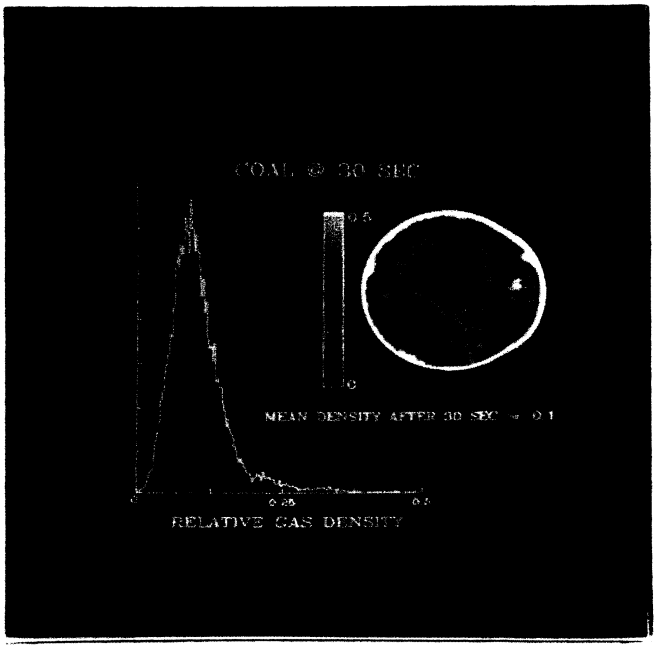

Figure 11

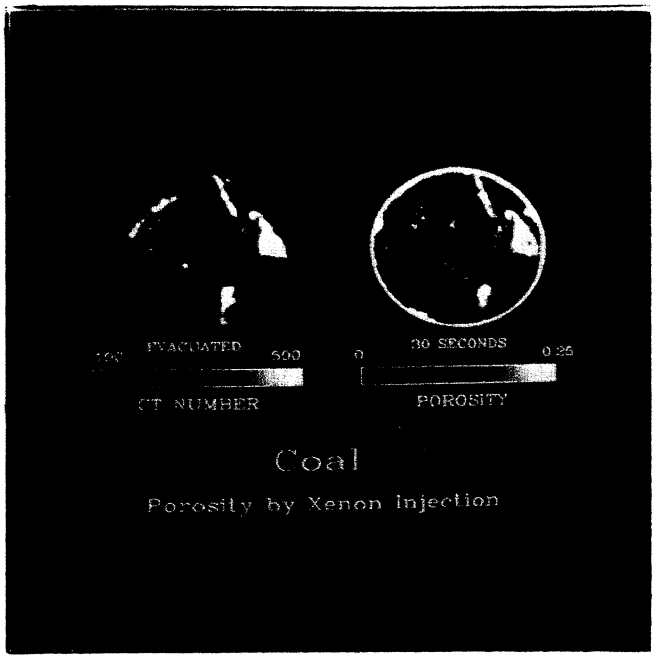

Figure 12

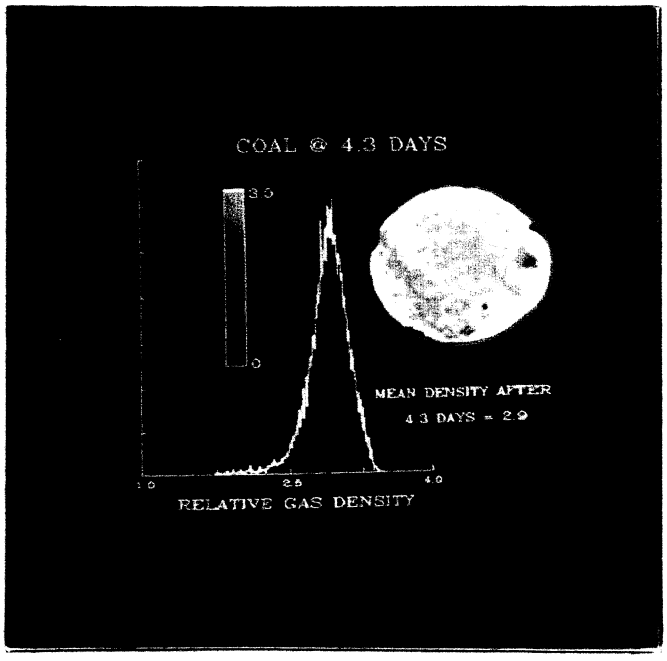

Figure 13